

## FOURIER TRANSFORM SPECTROSCOPY OF THE SWAN ( $d^3\Pi_g-a^3\Pi_u$ ) SYSTEM OF THE JET-COOLED C<sub>2</sub> MOLECULE

C. V. V. PRASAD<sup>1</sup> AND P. F. BERNATH<sup>2</sup>

Centre of Molecular Beams and Laser Chemistry, Department of Chemistry, University of Waterloo, Waterloo, Ontario, Canada N2L 3G1

Received 1993 May 24; accepted 1993 November 15

### ABSTRACT

The Swan ( $d^3\Pi_g-a^3\Pi_u$ ) system of the C<sub>2</sub> molecule was produced in a jet-cooled corona excited supersonic expansion of helium using diazoacetonitrile as a precursor molecule. This spectrum was recorded using the McMath Fourier transform spectrometer of the National Solar Observatory at Kitt Peak. A total of nine bands with  $v' = 0$  to 3 and  $v'' = 0$  to 4 in the range 16,570–22,760 cm<sup>-1</sup> were observed and rotationally analyzed. The C<sub>2</sub> molecules in this source had a rotational temperature of only 90 K so that only the low- $J$  lines were present in the spectrum. In some sense the low temperatures in the jet source simulate conditions in the interstellar medium. The Swan system of C<sub>2</sub> was also produced in a composite wall hollow cathode made Al<sub>4</sub>C<sub>3</sub>/Cu, and the rotational structure of the 1–0, 2–1, 3–2, 0–0, and 1–1 bands were analyzed. The data obtained from both these spectra were fitted together along with some recently published line positions. The rotational constants, lambda doubling parameters and the vibrational constants were estimated from this global fit. Our work on jet-cooled C<sub>2</sub> follows similar work on the violet and red systems of CN. A summary of this CN work is also presented.

*Subject headings:* molecular data — techniques: spectroscopic

### 1. INTRODUCTION

Diatomeric carbon C<sub>2</sub> and the CN free radical are prominent constituents of many extraterrestrial sources and thus are molecules of great astrophysical significance. Very intense visible bands observed in the heads of some comets are mainly due to the Swan ( $d^3\Pi_g-a^3\Pi_u$ ) system of C<sub>2</sub>, the violet ( $B^2\Sigma^+-X^2\Sigma^+$ ) and the red ( $A^2\Pi_u-X^2\Sigma^+$ ) systems of CN. The Swan bands of C<sub>2</sub> are also identified in the spectra of the Sun and late-type stars. In R- and N-type stars, the Swan bands of C<sub>2</sub> and the red bands of CN appear with such great intensity that these types of stars are also known as carbon stars.

The C<sub>2</sub> molecule is found in a variety of celestial sources such as comets (Mayer & O'Dell 1968; Johnson, Fink, & Larson 1983; Lambert & Danks 1983; Gredel, van Dishoeck, & Black 1989), interstellar clouds (Souza & Lutz 1977; Chaffee & Lutz 1978; Hobbs 1979; Hobbs & Campbell 1982; Chaffee et al. 1980; Hobbs 1981; van Dishoeck & de Zeeuw 1984; Hobbs, Black, & van Dishoeck 1983; Federman & Huntress 1989), the Sun (Grevesse & Sauval 1973; Brault et al. 1982; Lambert 1978), and in stellar atmospheres (Querci, Querci, & Kunde 1971; Goebel et al. 1983). The  $\Delta v = \pm 1$  sequences of the Swan band system of the C<sub>2</sub> molecule were recorded by Lambert & Danks (1983) in emission from Comet West 1976 VI. They also observed a few lines of the 0–0 band of this system for <sup>12</sup>C<sub>2</sub> and <sup>12</sup>C<sup>13</sup>C. The C<sub>2</sub> molecule was also detected in the interstellar medium. For example, the 2–0 band of the Phillips ( $A^1\Pi_u-X^1\Sigma_g^+$ ) system of C<sub>2</sub> was recorded in the interstellar medium toward the bright stars  $\zeta$  Ophiuchi (Chaffee & Lutz 1978),  $\zeta$  Persei (Hobbs 1979; Chaffee et al. 1980), a late B star HD 29647 (Hobbs et al. 1983),  $\sigma$  Persei (Hobbs 1981), and  $\chi$  Ophiuchi, HD 154368, and HD 147889 (van Dishoeck & de Zeeuw 1984). The 1–0 band of this system was detected in the near-infrared spectrum of Cygnus OB2 12

by Souza & Lutz (1977) and also in the solar photospheric spectrum (Brault et al. 1982). Brault et al. (1982) also observed the 0–0 and 0–1 bands of this system. Goebel et al. (1983) detected the  $\Delta v = 0$  sequence of the Phillips band system of C<sub>2</sub> and the  $\Delta v = -3$  sequence of the red system of CN in the spectrum of the R-type carbon star HD 19557. The studies of the interstellar spectra of the Swan and Phillips systems of the <sup>12</sup>C<sub>2</sub> and <sup>12</sup>C<sup>13</sup>C molecule are convenient for the estimation of the <sup>12</sup>C/<sup>13</sup>C abundance ratio (Stawikowski & Greenstein 1964; Danks, Lambert, & Arpigny 1974; Lambert & Danks 1983).

The CN radical was also detected in a variety of celestial sources such as the Sun (Lambert 1968; Sneden & Lambert 1982), stellar atmospheres (Lambert et al. 1984; Wootten et al. 1982), comets (Johnson et al. 1983), dark interstellar clouds (Turner & Gammon 1975; Gerin et al. 1984), and diffuse interstellar clouds (Meyer & Jura 1984, 1985; Morton 1975; Lambert, Sheffer, & Crane 1990; Federman, Danks, & Lambert 1984; Crane et al. 1986; Black & van Dishoeck 1988; Meyer, Roth, & Hawkins 1989).

After the discovery of the 3 K cosmic background radiation (Penzias, Jefferts, & Wilson 1972), it was realized that the rotational energy level spacing of CN is ideal for the measurement of cosmic temperatures (Thaddeus 1972). For example, the relative population of the  $N = 1$  and  $N = 0$  levels of CN as measured by optical absorption, gives a temperature of  $2.83 \pm 0.09$  K (Meyer et al. 1989) in good agreement with value of 2.3 K derived by McKellar (1941). McKellar (1940) was first to identify the lines of the CN violet system observed in diffuse interstellar clouds by Adams (1941). Recently Prasad et al. (1992) listed improved estimates for the line position of the observed or potentially observable interstellar absorption lines. These measurements were made by jet-cooling the CN radical in an expansion into vacuum, similar to the work on C<sub>2</sub> reported here.

Even though the CN and C<sub>2</sub> molecules have been investigated thoroughly for more than a century both in the labor-

<sup>1</sup> Postal address: Department of Chemistry, University of Victoria, Victoria, B.C., Canada V8W 3P6.

<sup>2</sup> Also Department of Chemistry, University of Arizona, Tucson, AZ 85721.

atory and in the extraterrestrial sources, there has been a renewed interest in these molecules with the development of new experimental techniques. The 0–1 (Curtis & Sarre 1985) and 1–0 (Suzuki, Saito, & Hirota 1985) bands of the Swan system of  $C_2$  were recorded using laser excitation spectroscopy. The violet and the red systems of CN were recently recorded in emission with a Fourier transform spectrometer using the corona-excited supersonic jet expansion technique (Prasad & Bernath 1992; Prasad et al. 1992, Rehfuss et al. 1992; Richard, Donaldson, & Vaida 1989). The molecules produced using this jet expansion technique are rotationally cold (30–50 K) but vibrationally hot (2000–6000 K). The molecules are excited to very high vibrational levels but for each vibrational level only a few low-lying rotational levels are populated, thus giving rise to a spectrum with only a few low- $J$  rotational lines. These low- $J$  lines are often too weak and blended to be observed in traditional high temperature sources. In the jet source these few rotational lines are, in general, very sharp and well resolved, as well as free from local perturbations. Accurate  $T_v$ - and  $B_v$ -values for a large number of vibrational levels can be estimated, and this in turn is useful for the construction of RKR potential energy curves and the calculation of Franck-Condon factors.

The low temperature emission spectra are ideal for the precise determination of the line positions. In some sense the jet expansion technique provides experimental conditions which simulate the cold conditions of interstellar space where the CN and  $C_2$  molecules are abundant. The jet source complements the traditional high-temperature laboratory sources of  $C_2$  and CN such as carbon arcs, flames and electrical discharges. These sources provide data extending to much higher rotational levels but the low- $J$  spectral lines are almost always blended. The relatively narrow linewidth and freedom from blending makes the jet source data a valuable addition to the extensive data sets produced by high temperature sources of CN and  $C_2$ . In the present work the Swan system of  $C_2$  produced in a jet source was recorded using McMath Fourier transform spectrometer of National Solar Observatory at Kitt Peak and the results of the analysis of the spectra are reported in this paper.

## 2. PAST AND PRESENT WORK

The Swan band system of  $C_2$  has been investigated numerous times since the work of Wollaston (1802) and Swan (1857) almost two centuries ago. The literature on the Swan system is enormous. There was controversy about the emitter of the band system until King & Birge (1930) analyzed the Swan bands of the  $^{12}C^{13}C$  molecule. The vibrational analysis of the main bands of the system was given by Mecke (1925), Johnson (1927) and Shea (1927). Herzberg (1946) correctly identified the high pressure bands of  $C_2$  to be the  $v' = 6$  progression of the Swan system, and Phillips (1948) observed and identified several “tail” bands of this system. Many early investigators including Shea (1927), Budó (1936), and Mulliken (1927, 1929) attempted the rotational analysis of these bands. Although Johnson & Asundi (1929) and Ciccone (1942) measured the rotational structure of some of the high-pressure bands, a complete rotational analysis was not published. Phillips (1948) performed the rotational analysis of the tail bands of this system and later Burgrim et al. (1965) observed four more bands. Phillips & Davis (1968) published a complete atlas of the Swan system of  $C_2$  listing extensive rotational data for 35 bands with  $v' = 0$  to 6 and 8 to 10 and  $v'' = 0$  to 9. They discussed the

perturbations (also see Phillips 1968) and presented vibrational and rotational constants for the  $a^3\Pi_u$  and  $d^3\Pi_g$  states. Although their data were very extensive, the accuracy of the line positions can be improved by modern laser and Fourier transform techniques. For all of the literature prior to 1977 the reader is referred to Huber & Herzberg (1979) and Tyte, Innanen, & Nicholls (1967).

Recently Amiot (1983) investigated the 0–0 band of the Swan system of  $^{12}C_2$ ,  $^{13}C_2$ , and  $^{12}C^{13}C$  produced in an electrodeless microwave discharge using a Fourier transform spectrometer. Curtis & Sarre (1985) and Suzuki et al. (1985) investigated the 0–1 and 1–0 bands, respectively, of this system of  $^{12}C_2$  using the technique of laser excitation spectroscopy. Curtis & Sarre (1988) also measured the hyperfine structure of  $^{13}C_2$  by the nonlinear laser technique of intermodulated fluorescence. Li & Francisco (1992) reported the observation of the 2–0, 1–0, and 0–0 bands of the Swan system produced by the infrared multiphoton dissociation of bistrifluoromethyl peroxide. More recently in our laboratory, Douay, Niemann, & Bernath (1988a, b) observed some new bands of the Phillips ( $A^1\Pi_u - X^1\Sigma_g^+$ ) system of  $C_2$  and also discovered two new infrared transitions,  $B'^1\Sigma_g^+ - A^1\Pi_u$  and  $B^1\Delta_g - A^1\Pi_u$ , of this molecule. Davis et al. (1988a, b) reinvestigated the Ballik-Ramsay ( $b^3\Sigma_g^- - a^3\Pi_u$ ) and the Phillips systems.

In the present work, nine bands (0–1, 1–2, 2–3, 3–4, 0–0, 1–1, 1–0, 2–1, and 3–2) of the Swan system of  $C_2$  were produced in a jet source and the spectra were recorded with a Fourier transform spectrometer. The 0–0, 1–1, 1–0, 2–1, and 3–2 bands produced in a hollow cathode discharge were also recorded on the same spectrometer. The details of the experimental work and the results of the analysis of all these bands, along with the most recent data on the Swan system of  $^{12}C_2$  are presented in §§ 3 and 4, respectively. A brief summary of this work is given in § 5.

## 3. EXPERIMENTAL DETAILS

The Swan ( $d^3\Pi_g - a^3\Pi_u$ ) system of the  $C_2$  molecule was produced in a jet-cooled corona excited supersonic expansion of the type proposed by Engelking (1986). A potential of 3.5 kV was applied through a ballast resistor of  $2\text{ M}\Omega$  to a tungsten wire of  $250\text{ }\mu\text{m}$  diameter. This tungsten wire is placed inside a quartz tube of 6 mm outer diameter and is  $400\text{ }\mu\text{m}$  from the  $250\text{ }\mu\text{m}$  diameter pinhole nozzle. Diazoacetonitrile was used as the precursor molecule for the production of  $C_2$  molecules and helium at a pressure of 4 atm was used as the carrier gas. The  $C_2$  molecule was found in a series of experiments designed to look for the HCCN and CCN free radicals (Oliphant et al. 1990). The pressure in the vacuum chamber was several hundred mTorr. The potential drop through the nozzle provided the electrical excitation to form a plasma. The subsequent free jet expansion collisionally cooled the rotational motion of the molecules.

The radiation emitted by the rotationally cooled but electronically excited molecules was recorded by focusing the emission perpendicular to the molecular jet onto the entrance aperture of the McMath Fourier transform spectrometer of the National Solar Observatory at Kitt Peak. A total of four scans were co-added in 18 minutes of integration at a resolution of  $0.025\text{ cm}^{-1}$ . Cooled GaAs photomultiplier tube detectors were used along with a  $4300\text{ \AA}$  red-pass and a  $6000\text{ \AA}$  blue-pass filter. This selection of filters and detectors allowed the spectrum to be recorded in the  $16,000\text{--}23,000\text{ cm}^{-1}$  region.

In this spectrum several bands of the red ( $A^2\Pi_u - X^2\Sigma^+$ )

system of the CN molecule (Prasad & Bernath 1992) and also those of the  $\tilde{A}^2\Delta-\tilde{X}^2\Pi$  system of CCN (Oliphant et al. 1990) were observed. For absolute wavenumber calibration, the data from Doppler-limited dye laser studies of Kakimoto & Kasuya (1982) on CCN were compared with those observed in our spectrum. As a double check, the spectral lines due to  $C_2$  were compared with those of Suzuki et al. (1985) and Curtis & Sarre (1985) and the spectral line positions were found to be in good agreement.

In order to increase the number of rotational lines in our data set some additional spectra of the Swan system were analyzed. The Swan system of  $C_2$  was produced in a composite-wall hollow cathode, made of  $Al_4C_3$  and Cu. Argon gas at a pressure of 1.5 Torr was used as carrier gas and applied voltage of 400 V produced a discharge current of 400 mA. Eighteen scans were co-added in 45 minutes of integration at a resolution of  $0.05\text{ cm}^{-1}$ . GaAs photomultiplier tube detectors, when used along with the 4000 Å red-pass and a 5500 Å blue-pass filters, limited the spectral region to  $17,770-21,937\text{ cm}^{-1}$ . These spectra were recorded in an unsuccessful attempt to observe AlC. The spectrum recorded from the hollow cathode source was calibrated with the help of argon lines present in the spectrum using the line positions reported by Norlen (1973). After this calibration the data from the hollow cathode source were found to be on the same wavenumber scale as the data from the jet source.

The rotational temperature in the hollow cathode source (just above room temperature) is relatively higher than in the jet source (about 90 K), thereby allowing the observation of transitions with higher  $J$ -values. However, the spectral lines obtained from the jet source are much sharper and the spectrum is less congested. A part of the 0-0 band of the Swan system of the  $C_2$  molecule recorded in the jet and the hollow cathode sources are compared in Figure 1. For the sake of clarity only a few spectral lines in some of the branches are identified in this spectrum. The clearly demonstrates the usefulness of the jet source in producing simpler spectra of molecules. In the jet spectrum, because the strong  $P$  branch lines returning from the head are absent, two  $Q$  branches can be clearly seen (Fig. 1). These  $Q$  branches could not be identified in the spectrum recorded from the hollow cathode source

because the weak first rotational lines of the  $Q$  branches are overlapped by the strong lines of the  $P$  branches. Because of the very low rotational temperature ( $\sim 90$  K) of the  $C_2$  molecules in the jet source, only lines with  $J \leq 9$  are observed. At the higher temperature in the hollow cathode source, spectral lines with  $J \leq 30$  are typically observed.

#### 4. ANALYSIS OF THE SPECTRA

The Swan system of the  $C_2$  molecule is a  $^3\Pi-^3\Pi$  electronic transition with each state nominally obeying Hund's case (b) coupling at high  $J$ -values. In such a transition three strong  $P$  branches and three strong  $R$  branches are expected (Herzberg 1950). Three very weak  $Q$  branches are also possible but their intensity decreases rapidly with increasing  $J$ . There are three distinct types of bands in the Swan system, known as the "head" bands or main bands, the "tail" bands, and the high-pressure bands. The main bands are degraded to shorter wavelengths, occur in the region  $4350-6680\text{ \AA}$  and are most commonly observed. The high pressure bands are the  $v' = 6$  progression (Herzberg 1946) containing eleven bands degraded to shorter wavelengths and occurring in the region  $3400-7850\text{ \AA}$ . Of the 10 known tail bands of the Swan system, three are headless and the rest are degraded to longer wavelengths. They occur in the  $4100-5000\text{ \AA}$  region and involve high vibrational quantum numbers (Tyte et al. 1967).

As an illustration, the 0-0 and 1-0 bands of the Swan system produced in the jet source are shown in Figures 2 and 3, respectively. In addition to the three  $P$  and three  $R$  branches,  $Q_1$  and  $Q_2$  branches can also be seen in these two spectra. Transitions taking place between the  $F_1$  spin components are the strongest, i.e., the  $P_1$ ,  $Q_1$ , and  $R_1$  are very strong and those between the  $F_3$  spin components are the weakest. The  $Q_3(J)$  transitions, being much weaker than the  $Q_2(J)$ , could not be observed in these spectra. The low temperature of our jet expansion has cooled most of the population out of the  $F_3$  spin component of the  $d^3\Pi_g$  state. With a spin-orbit coupling constant of about  $-15\text{ cm}^{-1}$  for both states and a rotational constant of about  $1.6\text{ cm}^{-1}$ , both  $^3\Pi$  states obey Hund's case (a) coupling at low  $J$ .

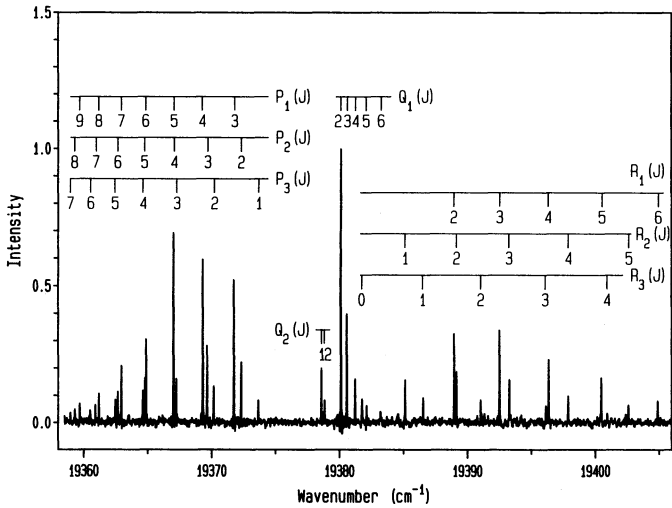


FIG. 2.—Rotational structure of the 0-0 band of the Swan system of the  $C_2$  molecule produced in the jet source using diazoacetonitrile as a precursor molecule.

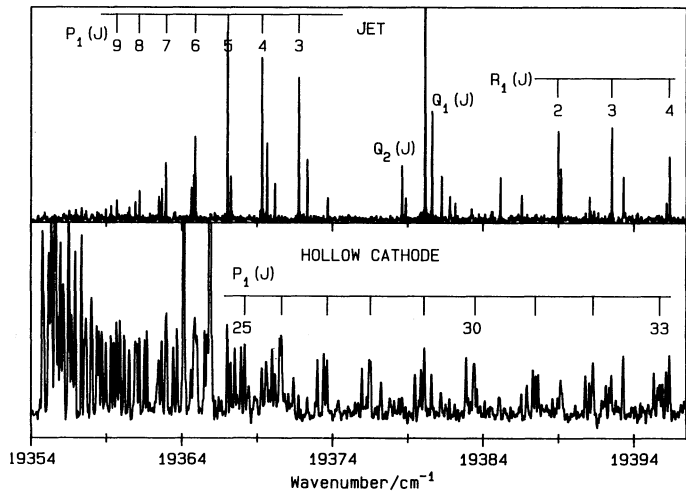


FIG. 1.—Part of the 0-0 band of the Swan ( $d^3\Pi_g-a^3\Pi_u$ ) system of the  $C_2$  molecule produced in the jet and the hollow cathode sources. For the sake of clarity only a few spectral lines are identified in these spectra.

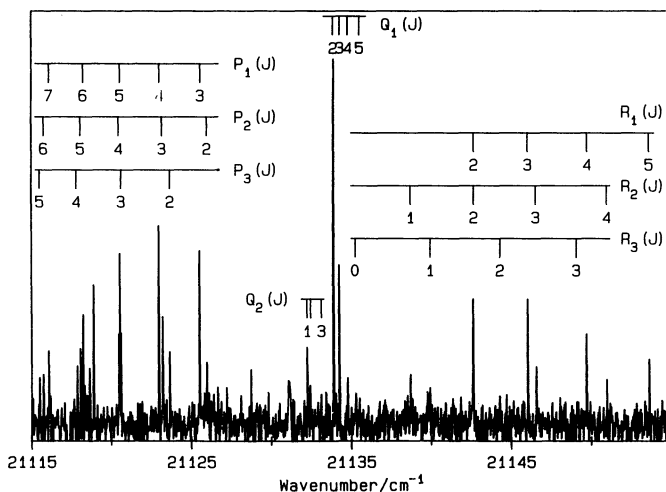


FIG. 3.—Rotational structure of the 1-0 band of the Swan system of the  $\text{C}_2$  molecule produced in the jet source using diazoacetonitrile as a precursor molecule.

In some laser spectroscopic studies of the Swan system of  $\text{C}_2$  by Curtis & Sarre (1985) and Suzuki et al. (1985), in addition to the regular transitions with  $\Delta\Omega = 0$ , a few cross (satellite) transitions with  $\Delta\Omega = \pm 1$  were also observed. The transitions with  $\Delta\Omega = \pm 1$  were found only by laser spectroscopy and they were not observed in the present work or in the previous Fourier transform work by Amiot (1983). Although the low- $J$  transitions belong to Hund's case (a), the molecule rapidly switches to Hund's case (b) with increasing rotation. This change from Hund's case (a) to Hund's case (b) can be clearly seen in the  $P$  branches of the 0-0 band in Figure 2. Initially at low  $J$  the spectral lines of the three spin components are far apart but they become closer and cross near  $N = 4$ . The transition to case (b) is occurring there and thereafter the typical triplets of a Hund's case (b)  $^3\Pi - ^3\Pi$  transition are found. The spectral lines in the  $R$  branches are farther apart and hence the transition from case (a) to case (b) is not as clear.

The  $\text{C}_2$  molecule is a homonuclear diatomic and the nuclear spin,  $I$ , of carbon is zero, so that the antisymmetric (a) energy levels are not populated (Herzberg 1950). Since the s/a symmetry (associated with the permutation of the two identical nuclei) alternates with  $J$ , every alternate spectral line is missing in the spectrum. For a  $^3\Pi - ^3\Pi$  transition this effect is not obvious because of the twofold orbital degeneracy of the  $\Pi$  states. In this case one of the two  $\Lambda$ -doublets is missing for each  $J$  and, apart from the slight "staggering" of the lines in a branch, the spectrum has a normal appearance. In  $P$  and  $R$  branches the spectral lines with even  $J$  numbers represent  $f \rightarrow f$  transitions and those with odd  $J$  numbers represent  $e \rightarrow e$  transitions. In  $Q$  branches, the spectral lines with even  $J$  numbers represent  $e \rightarrow f$  transitions and those with odd  $J$  numbers represent  $f \rightarrow e$  transitions. For the sake of clarity, the parities are not marked on the spectra shown in Figures 1 to 3.

The computer program PC-DECOMP, developed by J. W. Brault at the National Solar Observatory, was used to measure the line positions. The rotational line profiles were fitted to Voigt line shape functions. The strong lines show "ringing" caused by the  $(\sin x/x)$  line shape function of the Fourier transform spectrometer. The ringing was eliminated by using the "filter fitting" option of PC-DECOMP. The signal-to-noise ratio for strong lines was about 20 for the jet spectrum and about 10 for the hollow cathode spectrum. The rotational quantum numbers and the vacuum wavenumbers of the spectral lines of all the bands observed in the jet and hollow cathode sources are listed in Tables 1 and 2, respectively.

Initially band-by-band fits of the wavenumber data of Tables 1 and 2 were made using the  $N^2$  Hamiltonian of Brown & Merer (1979) for  $^3\Pi$  states. The matrix elements of this effective Hamiltonian are explicitly listed by Brown & Merer (1979) and Brazier, Ram, & Bernath (1986). For the final least-squares fit, the wavenumber data listed in Tables 1 and 2 were combined with those of Curtis & Sarre (1985) for the 0-1 band, Suzuki et al. (1985) for the 1-0 band, and Amiot (1983) for the 0-0 band. The data of Curtis & Sarre (1985) and Suzuki et al. (1985) contained some cross-transitions between the  $F_1 \rightarrow F_2$ ,  $F_2 \rightarrow F_1$ ,  $F_2 \rightarrow F_3$  and  $F_3 \rightarrow F_2$  levels. These data are useful in

TABLE 1

VACUUM WAVENUMBERS<sup>a,b</sup> (IN  $\text{cm}^{-1}$ ) FOR THE ROTATIONAL LINES OF THE BANDS OF THE SWAN ( $d^3\Pi_g - a^3\Pi_u$ ) SYSTEM OF THE  $\text{C}_2$  MOLECULE PRODUCED IN A JET SOURCE

$J$	$P_{11}(J)$	$P_{22}(J)$	$P_{33}(J)$	$R_{11}(J)$	$R_{22}(J)$	$R_{33}(J)$	$Q_{11}(J)$	$Q_{22}(J)$
0-1 Band								
0.....								
1.....								
2.....		17754.427(1)	17755.767(23)	17770.985(1)	17771.248(0)	17773.214(3)	17768.635(17)	17760.641(-3)
3.....	17753.851(5)	17751.848(8)	17749.532(7)	17774.609(2)	17775.489(11)	17778.438	17762.150(3)	17762.686(3)
4.....	17751.516(5)	17749.350(0)	17747.088(5)	17778.557(2)	17780.216(6)	17783.406(-8)	17763.440(6)	
5.....	17749.350(0)	17747.262(1)	17745.112(-8)	17782.820(5)		17789.007(-8)		
6.....	17747.381(3)	17745.336(-10)		17787.440(26)				
7.....	17745.640(2)	17743.835(13)		17792.334(8)				
8.....	17744.126(-1)							
1-2 Band								
1.....								
2.....		17913.452(-6)	17911.295(5)	17929.956(5)	17930.083(-3)	17931.917	17921.220(7)	17919.605(-9)
3.....	17912.999(7)	17910.883(0)	17908.505(25)	17933.523(4)	17934.239(-6)	17937.043(-13)	17921.732(2)	
4.....	17910.669(5)	17908.408(-3)		17937.407(4)	17938.912(-3)		17922.447(-5)	
5.....	17908.505(-1)	17906.325(6)		17941.588(-3)	17943.712(7)			
6.....	17906.534(3)							
7.....	17904.740(-42)							
8.....	17903.256(0)							

TABLE 1—Continued

<i>J</i>	<i>P</i> <sub>11</sub> ( <i>J</i> )	<i>P</i> <sub>22</sub> ( <i>J</i> )	<i>P</i> <sub>33</sub> ( <i>J</i> )	<i>R</i> <sub>11</sub> ( <i>J</i> )	<i>R</i> <sub>22</sub> ( <i>J</i> )	<i>R</i> <sub>33</sub> ( <i>J</i> )	<i>Q</i> <sub>11</sub> ( <i>J</i> )	<i>Q</i> <sub>22</sub> ( <i>J</i> )
2–3 Band								
1.....				18070.896(43)	18072.055(–8)			18064.562(83)
2.....	18058.475(93)	18056.186(–11)	18074.759(3)	18074.860(46)	18076.548(–5)	18066.107(–10)	18064.830(73)	
3.....	18057.963(–9)	18055.893(70)	18053.405(1)	18078.271(7)	18078.910(9)	18081.611	18066.599(–12)	
4.....	18055.649(–2)	18053.405(45)	18051.022(18)	18082.078(–3)	18083.475(–17)	18086.434(–17)	18067.297(–7)	
5.....	18053.499(7)	18051.275(10)			18088.138(–55)			
6.....	18051.506(–5)	18049.323(–22)						
7.....	18049.763(19)	18047.724(–56)						
8.....	18048.188(–9)							
3–4 Band								
2.....			18183.749(7)	18202.657(–11)			18194.149(–3)	
3.....	18186.084(–6)	18183.749(93)	18181.148(88)	18206.119(26)			18194.594(–12)	
4.....	18183.749(–9)							
5.....	18181.588(9)							
6.....	18179.558(–8)							
0–0 Band								
0.....					19381.791(15)			
1.....		19373.693(20)		19385.139(0)	19386.556(9)			
2.....	19372.329(0)	19370.171(4)	19388.976(5)	19389.152(1)	19391.054(11)	19380.138(4)	19378.613(2)	
3.....	19371.763(6)	19369.655(2)	19367.252(16)	19392.521(5)	19393.292(1)	19396.161(12)	19380.599(6)	
4.....	19369.317(4)	19367.024(–5)	19364.622(–3)	19396.360(2)	19397.898(8)	19400.963(6)	19381.242(6)	
5.....	19367.024(8)	19364.789(4)	19362.456(–11)	19400.481(–1)	19402.614(3)	19406.354(–8)	19382.150(12)	
6.....	19364.880(5)	19362.668(3)	19360.519(9)	19404.906(–4)	19407.678(5)		19383.227(9)	
7.....	19362.935(–3)	19360.930(14)	19358.962(–2)	19409.635(9)	19412.869(–31)			
8.....	19361.192(2)	19359.311(0)						
9.....	19359.699(13)							
1–1 Band								
0.....					19517.312(38)			
1.....		19509.262(16)		19520.742(33)	19521.978(10)			
2.....	19508.043(3)	19505.794(–4)	19524.625(3)	19524.664(–4)	19526.435(10)	19515.893(9)	19514.501(11)	
3.....	19507.590(6)	19505.379(3)	19502.858(–17)	19528.118(7)	19528.746(8)	19531.451(0)	19516.326(4)	
4.....	19505.153(3)	19502.786(16)	19500.307(10)	19531.895(7)	19533.274(0)	19536.216(15)	19516.938(0)	
5.....	19502.858(3)	19500.526(4)	19498.133	19535.944(4)	19537.947(39)		19517.834(30)	
6.....	19500.715(4)	19498.432(21)	19496.179(–8)	19540.296(6)				
7.....	19498.775(12)	19496.633(–9)						
8.....	19496.993(–10)	19495.054(22)						
1–0 Band								
0.....					21135.247(8)			
1.....					21139.899(2)			
2.....	21125.961(19)	21123.660(30)	21142.615(5)	21142.615(45)	21144.230(–28)	21133.881(9)	21132.395(2)	
3.....	21123.194(5)	21120.600(14)	21146.031(10)	21146.573(22)	21149.173(11)	21134.235(2)	21133.394(28)	
4.....	21122.961(10)	21120.459(10)	21117.867(27)	21149.690(0)	21150.964(11)		21134.746(6)	
5.....	21120.523(2)	21118.069(23)	21115.483(3)	21153.608(1)	21155.467(36)		21135.491(20)	
6.....	21118.211(3)	21115.728(–1)	21113.331(33)	21157.790(3)	21160.239(22)			
7.....	21116.076(15)	21113.726(–10)		21162.232(16)				
8.....	21114.076(10)							
2–1 Band								
0.....					21233.374(–5)			
1.....		21225.392(–4)		21236.891(75)	21237.939(–9)			
2.....	21224.317(95)	21221.886(–16)	21240.751(–14)	21240.696(43)	21242.259(1)	21232.119(–6)	21230.668(72)	
3.....	21223.815(–10)	21221.558(77)	21218.859(3)	21244.120(3)	21244.575(15)	21247.054(–9)	21232.464(–1)	
4.....	21221.290(–1)	21218.800(44)	21216.130(1)	21247.720(–1)	21248.858(–30)	21251.571(–7)	21232.944(0)	
5.....	21218.859(–1)	21216.364(20)	21213.786(41)	21251.565(9)	21253.275(3)			
6.....	21216.548(4)	21213.976(–49)		21255.646(–9)				
7.....	21214.398(19)			21259.996(16)				
3–2 Band								
0.....					21314.143(28)			
1.....					21318.663(–35)			
2.....	21305.334(–35)	21302.805(34)	21322.000(–1)	21321.555(–16)	21322.892(16)	21313.492(6)	21311.658(–4)	
3.....	21305.268(4)	21302.625(–10)	21299.875(51)	21325.300(32)	21325.418(12)		21313.778(–1)	
4.....	21302.713(–1)	21299.875(–20)	21297.059(21)	21328.772(2)	21329.615(–5)		21314.233(31)	
5.....	21300.288(32)	21297.493(14)	21294.747(34)	21332.542(44)			21314.822(–2)	
6.....	21297.944(45)	21295.110(–5)						
7.....	21295.731(42)	21293.119(42)						

<sup>a</sup> The number in the parentheses indicates  $(v_{\text{obs}} - v_{\text{calc}}) \times 10^3$  in  $\text{cm}^{-1}$  units. If this number is not given, then the listed number is a calculated wavenumber.

<sup>b</sup> In *P* and *R* branches the spectral lines with odd *J*-values represent an *e* → *e* transition and those with even *J*-values represent an *f* → *f* transition. In the case of *Q* branch, the transitions with odd *J*-values represent an *f* → *e* transition and those with even *J*-values represent an *e* → *f* transition.

TABLE 2

VACUUM WAVENUMBERS<sup>a,b</sup> (IN cm<sup>-1</sup>) FOR THE ROTATIONAL LINES OF THE BANDS OF THE SWAN ( $d^3\Pi_g-a^3\Pi_u$ ) SYSTEM OF THE C<sub>2</sub> MOLECULE PRODUCED IN A HOLLOW CATHODE DISCHARGE

<i>J</i>	<i>P</i> <sub>11</sub> ( <i>J</i> )	<i>P</i> <sub>22</sub> ( <i>J</i> )	<i>P</i> <sub>33</sub> ( <i>J</i> )	<i>R</i> <sub>11</sub> ( <i>J</i> )	<i>R</i> <sub>22</sub> ( <i>J</i> )	<i>R</i> <sub>33</sub> ( <i>J</i> )
0–0 Band						
0 .....			19373.642(–31)			19381.776(0)
1 .....		19372.335(6)	19370.11(23)			19386.527(–19)
2 .....	19371.759(3)	19369.616(–38)	19367.240(4)	19392.499(–18)	19393.292(1)	19391.047(4)
3 .....	19369.314(1)	19367.024(–5)	19364.614(–10)	19396.364(7)	19397.899(9)	19400.953(–3)
4 .....	19367.024(8)	19364.781(–4)	19362.463(–4)	19400.482	19402.605(–6)	19406.358(–4)
5 .....	19364.879(4)	19362.665(1)	19360.509(–1)	19404.909(–2)	19407.670(–3)	19411.566(3)
6 .....	19362.917(–20)	19360.909(–7)	19358.968(4)	19409.609(–16)	19412.898(–2)	19417.332(0)
7 .....	19361.191(2)	19359.309(–2)	19357.556(–2)	19414.614(1)	19418.404(–3)	19422.967(–2)
8 .....	19359.688(2)	19358.019(–39)	19356.507(–43)	19419.899(1)	19424.110(–1)	19429.165(16)
9 .....	19358.387(5)	19356.940(–17)	19355.608(–47)	19425.410(0)	19430.074	19435.236(–4)
10 .....	19357.358(9)	19356.151(–42)	19355.179(21)	19431.249(5)	19436.243(–5)	19441.860(0)
11 .....	19355.608(–2)	19355.608(19)	19354.760(0)	19437.260(4)	19442.681	19448.414(3)
12 .....	19355.507(36)	19356.507(36)	19356.940(10)	19471.389(3)	19478.286(–7)	19485.548(1)
13 .....	19355.953(–13)	19355.353(44)	19354.760(–4)	19443.645(22)	19449.318(–2)	19445.484(–5)
14 .....	19355.608(12)	19355.179(–24)	19354.851(–3)	19450.116(–2)	19456.236(2)	19462.500(–1)
15 .....	19355.608(56)	19355.353(–49)	19355.353(–3)	19457.012(3)	19463.331(–2)	19470.048(–2)
16 .....	19355.608(–47)	19355.795(1)	19355.953(23)	19463.986(9)	19470.733(–1)	19477.502(–2)
17 .....	19356.151(36)	19356.507(36)	19356.940(10)	19471.389(3)	19478.286(–7)	19485.548(1)
18 .....	19356.701(11)	19357.358(–7)	19358.019(35)	19478.823(4)	19486.182(–1)	19493.489(11)
19 .....	19357.660(4)	19358.516(1)	19359.487(4)	19486.746(4)	19494.184(–14)	19501.971(–14)
20 .....	19358.705(2)	19359.908(–5)	19361.014(–2)	19494.636(2)	19502.586(3)	19510.369(–2)
21 .....	19360.189(10)	19361.533(–2)	19362.997(–18)	19503.067(–1)	19511.041(–10)	19519.369(6)
22 .....	19361.702(8)	19363.440(2)	19365.009(–13)	19511.422(8)	19519.928(–3)	19528.196(–8)
23 .....	19363.694(14)	19365.526(–4)	19367.522(–2)	19520.362(6)	19528.828(–19)	19537.675(–8)
24 .....	19365.658(–7)	19367.935(–6)	19369.997(–7)	19529.161(10)	19538.216(–9)	19546.968(–5)
25 .....	19368.175(12)	19370.497(–5)	19373.008(–2)	19538.609(7)	19547.580(–7)	19556.971(28)
26 .....	19370.618(4)	19373.426(5)	19375.961(0)	19547.836(–7)	19557.459(–4)	19566.686(7)
27 .....	19373.642(16)	19374.643(–11)	19379.477(4)	19557.818(17)	19567.297(30)	19577.135(–6)
28 .....	19376.534(–6)	19379.881(3)	19382.888(–4)	19567.514(30)	19577.637(–5)	19587.322(1)
29 .....	19380.100(34)	19383.367	19386.921(11)	19577.952(5)	19587.886(0)	19598.259(–14)
30 .....	19383.420(–23)	19387.315(4)	19390.791(–4)	19588.080(12)	19598.752(–7)	19608.891(–3)
31 .....	19387.487(2)	19391.286(25)	19395.232(1)	19599.055(19)	19609.436(–2)	19620.386(48)
32 .....	19391.286(–36)	19395.728(10)	19399.672	19609.600(8)	19620.812(1)	19631.389(–6)
33 .....	19395.902(21)	19400.129	19404.716(8)	19621.058(–6)	19631.931(8)	19643.364(32)
34 .....	19400.176	19405.092(–8)	19409.520	19632.048(–4)	19643.792(–2)	19645.832(9)
35 .....	19405.260(9)	19409.997(29)	19415.083(16)	19644.000(–26)	19655.347(13)	19667.244(9)
36 .....	19409.997(–6)	19415.453(–1)	19420.338(0)	19655.443(0)	19667.681(–24)	
37 .....	19415.613(17)	19420.791(14)	19426.395	19667.907(–12)		
38 .....	19420.791(–11)	19426.780	19432.124			
39 .....	19426.912	19432.560(4)	19438.714(22)			
40 .....	19432.560(–11)	19439.068(–7)	19444.850(–27)			
41 .....	19439.172(–27)	19445.307(5)	19541.948(–9)			
42 .....	19445.307(–2)	19452.307(–31)	19458.595			
43 .....	19452.431(–24)	19459.015(1)	19466.164(–23)			
44 .....	19459.015(1)	19466.563(–3)	19473.270(–6)			
45 .....	19466.653(–22)	19473.678(–10)				
46 .....	19473.678(–4)					
1–1 Band						
1 .....		19509.232(–14)				
2 .....		19505.798	19524.630(7)	19524.630(–38)		
3 .....		19502.855(–20)	19528.196(84)	19528.828(91)		
4 .....	19502.855(1)	19502.771(1)	19500.294(–3)	19531.888	19533.274	19356.176(–25)
5 .....	19500.504(–18)	19498.130(–3)	19498.130(–3)	19535.935(–6)	19537.928(20)	19541.545(28)
6 .....	19500.727(15)	19498.411(1)	19496.208(21)	19540.251(–39)	19542.898	19546.655(12)
7 .....	19498.761(–2)	19496.613(–29)	19494.636(17)	19544.934(17)	19547.995(–28)	19552.301(–8)
8 .....	19496.992(–11)	19495.140(108)	19493.217(13)	19549.820(7)	19553.422(–22)	19557.818(–36)
9 .....	19495.468(7)	19493.792(47)	19492.187(27)	19555.006(11)	19559.053(21)	19563.975(58)
10 .....	19494.184(37)	19492.634(9)	19491.176(–64)	19560.403	19564.891(–4)	19569.909(11)
11 .....	19493.040(–35)	19491.816(3)	19490.668(–23)	19566.144(26)	19570.966(28)	19576.387
12 .....	19492.187(–13)	19491.176(2)	19490.209(–43)	19572.009(–4)	19577.183(–75)	19582.812(0)
13 .....	19491.609(7)	19490.815(–17)	19490.209(21)	19578.268(21)	19583.759(9)	19589.744
14 .....	19491.176(–10)	19490.668(–7)	19490.209(–13)	19584.614(2)	19590.533	19596.601(–14)
15 .....	19491.089(19)	19490.815(16)	19490.668(27)	19591.333(–21)	19597.471(–4)	19603.994(–5)
16 .....	19491.089(–24)	19491.176(52)	19491.176(34)	19598.162(–16)	19604.717(–9)	19611.321(7)
17 .....	19491.486(–1)	19491.714(4)	19491.985(–57)	19605.412(–9)	19612.098(–14)	19619.160
18 .....	19491.985(–3)	19492.518(–1)	19493.040(31)	19612.699(2)	19619.838	19626.921(3)
19 .....	19492.848(–3)	19493.489(–78)	19494.394(2)	19620.386(–50)	19627.659(–6)	19635.215(–14)
20 .....	19493.792(–19)	19494.861	19495.822(1)	19628.089(–67)	19635.854(–13)	19643.364(–62)

TABLE 2—Continued

<i>J</i>	<i>P</i> <sub>11</sub> ( <i>J</i> )	<i>P</i> <sub>22</sub> ( <i>J</i> )	<i>P</i> <sub>33</sub> ( <i>J</i> )	<i>R</i> <sub>11</sub> ( <i>J</i> )	<i>R</i> <sub>22</sub> ( <i>J</i> )	<i>R</i> <sub>33</sub> ( <i>J</i> )
1–1 Band						
21 .....	19495.140(−27)	19496.347(−20)	19497.692(5)	19636.357(−33)	19644.134(3)	19652.194(−12)
22 .....	19496.613(32)	19498.130(−18)	19499.635(60)	19644.529(−20)	19652.811	19660.823(−16)
23 .....	19498.411(−19)	19500.112(3)	19501.971(44)	19653.266(−8)	19661.513(4)	19670.069(−21)
24 .....	19500.294(−3)	19502.369(−11)		19661.892(25)	19670.698(31)	19679.195(40)
25 .....	19502.586(−55)	19504.795		19671.040(−43)	19679.702(−94)	19688.812(−66)
26 .....	19504.958(−1)	19507.556		19680.127(23)	19689.375(−59)	19698.377(4)
27 .....	19507.799	19510.369(−52)		19689.715(−95)	19698.966(−22)	
28 .....	19510.587(23)	19513.635(−39)		19699.261(5)		
1–0 Band						
0 .....			21127.196(21)			21135.267(28)
1 .....		21125.939(−3)	21123.598(−32)	21142.524(14)	21142.557(−14)	21144.276(18)
2 .....	21125.470(−24)	21123.183(−7)	21120.642(56)	21146.038(17)	21146.559(7)	21149.178(16)
3 .....	21122.917(−35)	21120.442(−7)	21117.856(17)	21149.656(−34)	21150.965(11)	21153.781(37)
4 .....	21120.530(9)	21117.986(−60)	21115.504(24)	21153.632(25)	21155.435(3)	21158.877(13)
5 .....	21118.139(−69)	21115.735(6)	21113.285(−12)	21157.790(4)	21160.185(−32)	21163.775(21)
6 .....	21116.059(−3)	21113.723(−13)	21111.478(12)	21162.207(−10)	21165.124(7)	21169.130(−26)
7 .....	21114.086(20)	21111.839(−15)	21109.749	21166.858(−17)	21170.258(−9)	21174.375(−23)
8 .....	21112.276(−1)	21110.250(−25)	21108.392(17)	21171.817(20)	21175.579(18)	21180.136(4)
9 .....	21110.672(27)	21108.817	21107.036(−49)	21176.896(−4)	21181.086(−2)	21185.743(1)
10 .....	21109.284(36)	21107.633(−10)	21106.167(26)	21182.299(8)	21186.772(3)	21191.849(12)
11 .....	21108.006(7)	21106.616(13)	21105.244(−20)	21187.813(1)	21192.673(−13)	21197.834(10)
12 .....	21107.036(23)	21105.837(7)	21104.740	21193.655(−3)	21198.738(−10)	21204.334(39)
13 .....	21106.167(14)	21105.244(36)	21104.263(−4)	21199.589(10)	21205.097(31)	21210.649(−11)
14 .....	21105.582(−4)	21104.850(19)	21104.119(−43)	21205.877(8)	21211.500(−5)	21217.498(−23)
15 .....	21105.147(30)	21104.657(29)	21104.119(30)	21212.168(−13)	21218.206(−25)	21224.225(−35)
16 .....	21104.975(0)	21104.657(14)	21104.411(9)	21218.870(−39)	21225.053(8)	21231.525(6)
17 .....	21104.975(81)	21104.850(−12)	21104.722(−2)	21225.591(−10)	21232.191(10)	21238.622(−10)
18 .....	21105.147(−32)	21105.244(−23)	21105.468(13)	21232.767(3)	21239.383(17)	21246.274(−19)
19 .....	21105.468(−16)	21105.928(18)	21106.167(−3)	21239.854(24)	21246.887(−28)	21253.804(28)
20 .....	21106.167(−33)	21106.709(7)	21107.345(22)	21247.413(−11)	21254.472(5)	21261.831(−10)
21 .....	21106.926(36)	21107.751(−19)	21108.469(42)	21254.876(18)	21262.430(−3)	21269.687(−5)
22 .....	21108.006(−30)	21108.947	21110.002	21262.875(−6)	21270.361(15)	21278.150(−15)
23 .....	21109.109	21110.455(13)	21111.478(−14)	21270.675(−4)		
24 .....	21110.672(−16)	21112.039(39)	21113.446(−45)	21279.104(−26)		
25 .....	21112.143(3)	21113.904(−21)	21115.370(5)			
26 .....	21114.086(−67)	21115.846(−16)	21117.735(−54)			
27 .....	21115.962(−21)	21118.139(−78)				
28 .....	21118.429	21120.530(0)				
29 .....	21120.642(9)	21123.323(6)				
31 .....		21126.025(23)				
2–1 Band						
0 .....			21225.419(22)			21233.372(−7)
1 .....		21224.222(0)	21221.902(−1)	21240.746(−19)	21240.644(−10)	21242.255(−3)
2 .....	21223.804(−21)	21221.525(43)	21218.870(15)	21244.160(43)	21244.597(37)	21247.046(−17)
3 .....	21221.257(−34)	21218.870(114)	21216.125(−4)	21247.676(−45)	21248.882(−6)	21251.569(−9)
4 .....	21218.870(10)	21216.334(−11)	21213.728(−17)	21251.569(13)	21253.222(−50)	21256.576(−8)
5 .....	21216.547(3)	21213.990(−34)	21211.500(−62)	21255.646(−9)	21257.974(8)	21261.449(58)
6 .....	21214.387(8)	21212.033(27)	21209.741(56)	21259.972(−8)	21262.721(−37)	21266.658
7 .....	21212.341(−28)	21210.025(−75)	21208.023(72)	21264.502(−44)	21269.327(1533) <sup>c</sup>	21271.876(73)
8 .....	21210.549(12)	21208.533(52)	21206.555(47)	21269.327(−10)	21273.930(961) <sup>c</sup>	21277.459(82)
9 .....	21208.840(−40)	21208.355(1381) <sup>c</sup>	21205.222(33)	21274.221(−116) <sup>c</sup>	21278.709(352) <sup>c</sup>	21282.918(38)
11 .....	21207.376(−41)	21206.706(956) <sup>c</sup>	21204.201(50)	21279.642(72) <sup>c</sup>	21283.873(−36) <sup>c</sup>	21288.733(−56)
12 .....	21205.996(−138) <sup>c</sup>	21204.981(346) <sup>c</sup>	21203.255(21)	21284.804(−177) <sup>c</sup>	21289.537(−123) <sup>c</sup>	21294.677(18)
13 .....	21205.097(43) <sup>c</sup>	21203.825(23) <sup>c</sup>	21202.505(−84)	21289.954(−684) <sup>c</sup>	21295.726(141) <sup>c</sup>	21300.891(−26)
14 .....	21204.063(−90) <sup>c</sup>	21202.972(105) <sup>c</sup>	21202.068(1)	21296.456(11) <sup>c</sup>	21301.670(−37) <sup>c</sup>	21307.233(77)
15 .....	21202.775(−687) <sup>c</sup>	21202.775(142) <sup>c</sup>	21201.909(96)	21303.120(603) <sup>c</sup>	21308.077(72) <sup>c</sup>	21313.773(0)
16 .....	21202.972(27) <sup>c</sup>	21202.300(3) <sup>c</sup>	21201.658(−25)	21308.630(−76) <sup>c</sup>	21314.504(3) <sup>c</sup>	21320.430(47)
17 .....	21203.255(606) <sup>c</sup>	21202.300(59) <sup>c</sup>	21201.909(93)	21315.220(36) <sup>c</sup>	21321.880(71) <sup>c</sup>	21327.445(80)
18 .....	21202.505(−11) <sup>c</sup>	21202.300(6) <sup>c</sup>	21202.068(−9)	21321.531(−220) <sup>c</sup>	21328.083(4) <sup>c</sup>	21334.297(−47)
19 .....	21202.775(161) <sup>c</sup>	21203.255(631) <sup>c</sup>	21202.505(91)	21328.760(130) <sup>c</sup>	21335.004(−76) <sup>c</sup>	21341.652(−41)
20 .....	21202.972(106) <sup>c</sup>	21202.972(−94) <sup>c</sup>	21203.255(9)	21335.378(−191) <sup>c</sup>	21342.328(−4)	21348.968(−72)
21 .....	21203.381(22) <sup>c</sup>	21203.825(44) <sup>c</sup>	21204.201(49)	21343.055(212) <sup>c</sup>	21349.637(−97)	21356.770(11)
22 .....	21203.825(−168) <sup>c</sup>	21204.587(−26)	21205.222(34)	21350.130(−20) <sup>c</sup>	21357.576(11)	21364.475(4)
23 .....	21204.981(99) <sup>c</sup>	21205.698(−14)	21206.555(75)	21357.894(79) <sup>c</sup>	21365.070(−61)	21372.544(−16)
24 .....	21205.698(−200) <sup>c</sup>	21206.926(−8)	21207.788(−115)	21365.427(−59) <sup>c</sup>	21373.094(−44)	
25 .....	21207.251(69) <sup>c</sup>	21208.355(−61)	21209.577(−3)	21373.638(98) <sup>c</sup>		

## SPECTROSCOPY OF SWAN SYSTEM

819

TABLE 2—Continued

<i>J</i>	$P_{11}(J)$	$P_{22}(J)$	$P_{33}(J)$	$R_{11}(J)$	$R_{22}(J)$	$R_{33}(J)$
2–1 Band						
26 .....	21208.355(–223) <sup>c</sup>	21210.025(–2)	21211.402(15)			
27 .....	21210.549(292) <sup>c</sup>	21211.776(–114)	21213.468(18)			
28 .....	21211.931(–100) <sup>c</sup>	21213.990(100)	21215.639			
29 .....	21214.290(186) <sup>c</sup>	21216.125(–7)	21218.077(–11)			
30 .....	21216.125(–131) <sup>c</sup>	21218.606(84)	21220.662(5)			
31 .....	21218.870(148) <sup>c</sup>					
32 .....	21221.093(–156) <sup>c</sup>					
33 .....	21224.222(113) <sup>c</sup>					
34 .....	21226.790(–219) <sup>c</sup>					
35 .....	21230.511(251) <sup>c</sup>					
3–2 Band						
0 .....						21314.112(–2)
1 .....						21318.631(–67)
2 .....		21305.263(–106)	21302.796(25)	21322.074(72)	21321.531(–40)	21322.860(–16)
3 .....	21305.263(–1)	21302.566(–69)	21299.854(30)	21325.297(29)	21325.439(33)	21327.583(–82)
4 .....	21302.796(82)	21299.854(–41)	21297.032(–6)	21328.760(–11)	21239.619(0)	21332.103(73)
5 .....	21300.265(10)	21297.523(43)	21294.677(–36)	21332.525(27)	21333.923(8)	21336.974(–13)
6 .....	21297.892(–7)	21295.077(–39)	21292.452(5)	21336.454(–13)	21338.467(0)	21341.652(34)
7 .....	21295.726(37)	21293.077(1)	21290.591(1)	21340.692(26)	21343.226(78)	21346.681(–124)
8 .....	21293.615(0)	21291.072(–26)	21288.733(–13)	21345.031(–45)	21348.005(–12)	21351.741(–6)
9 .....	21291.763(41)	21289.446(12)	21287.291(1)	21349.767(44)	21353.044(–11)	21357.178(–33)
10 .....	21289.954(–20)	21287.815(–13)	21285.875(42)	21354.526(–13)	21358.203(–49)	21362.469(–13)
11 .....	21288.498(64)	21286.480(–54)	21284.648(–105)	21359.656(47)	21363.647(9)	21368.188(–67)
12 .....	21287.020(–11)	21285.329(34)	21283.703(34)	21364.807(2)	21369.199(24)	21373.873(12)
13 .....	21285.875(18)	21284.354(–8)	21282.918(–39)	21370.331(46)	21374.914(10)	
14 .....	21284.804(–2)	21283.529(38)	21282.203(–34)	21375.824(–19)		
15 .....	21284.014(8)	21282.918(1)	21281.926(36)			
16 .....	21283.304(–3)	21282.485(72)	21281.542(11)			
17 .....	21282.918(35)	21282.203(10)	21281.542(–7)			
18 .....	21282.485(–49)	21281.926(–133)	21281.542(–5)			
19 .....	21282.485(–4)	21282.203(12)	21281.926(–5)			
20 .....	21282.485(–3)	21282.485(58)	21282.203(–79)			
21 .....	21282.918(97)	21282.918(10)	21283.065(33)			
22 .....	21283.198(31)	21283.529(14)	21283.873(140)			
23 .....	21283.873(–7)	21284.354(12)	21284.804(–46)			
24 .....	21284.556(–12)	21285.329(8)	21285.875(–23)			
25 .....	21285.657(–3)	21286.480(–12)	21287.291(–93)			
26 .....	21286.672(–17)	21287.815(–28)	21288.733(–42)			
27 .....	21288.154(–6)	21289.446(92)	21290.591(–37)			
28 .....	21289.537(12)	21291.072(–7)	21292.452(91)			
29 .....		21292.909(–17)	21294.677(96)			
30 .....		21295.077(53)				

<sup>a</sup> The number in the parentheses indicates  $(v_{\text{obs}} - v_{\text{calc}}) \times 10^3$  in  $\text{cm}^{-1}$  units. If this number is not given then the listed number is a calculated wavenumber.

<sup>b</sup> The spectral lines with odd *J*-values represent an  $e \rightarrow e$  transition and those with even *J*-values represent an  $f \rightarrow f$  transition.

<sup>c</sup> In the 2–1 band spectral lines belonging to the  $P_{11}(J)$ ,  $P_{22}(J)$ ,  $R_{11}(J)$ , and  $R_{22}(J)$  branches are affected by the perturbations in the upper state. They are deweighted in the least-squares fit.

determining the spin-orbit coupling constants ( $A_v$ ) and lambda doubling parameters ( $o_v$ ,  $p_v$ ,  $q_v$ , etc.). The data of Amiot (1983) extend up to  $J = 70$  and are useful in determining the centrifugal corrections such as  $D_v$ ,  $H_v$ ,  $A_{Dv}$ ,  $o_{Dv}$ ,  $p_{Dv}$ , and  $q_{Dv}$ . All this experimental data, about 1830 transitions in all, were fitted together simultaneously in a nonlinear least squares fit and a set of 59 parameters were estimated. The variance of this global fit was 1.308. Because the data from the jet source covered only a few rotational levels and those from the hollow cathode source were limited in resolution and signal-to-noise ratio, it was necessary to fix certain parameters in order to obtain a reasonable fit for the data. The  $A_v$  and  $D_v$ -values for the  $v = 2$ , 3, and 4 levels of the  $a^3\Pi_u$  state were fixed to those given by Davis et al. (1988a). The molecular parameters  $A_{Dv}$ ,  $D_v$ ,  $q_v$ ,  $p_v$ , and  $\lambda_v$  for these levels were fixed to reasonable values based on their values for the  $v = 0$  and 1 levels. The  $o_v$ -value for the level  $v = 4$  was also fixed to a reasonable value. Similarly for the

upper  $d^3\Pi_g$  state, the parameters  $A_{Dv}$ ,  $p_v$ , and  $\lambda_v$  for the levels  $v = 2$  and 3 were fixed to the reasonable values based on their values for the  $v = 0$  and 1 levels. The fitted parameters, along with one standard deviation error, are listed in Tables 3 and 4 for the  $a^3\Pi_u$  and  $d^3\Pi_g$  states, respectively.

In Tables 1 and 2, the observed minus calculated values obtained for the line positions using the molecular parameters listed in Tables 3 and 4, are also listed. This value is not given for a few spectral lines which were not in the fit and in this case only a calculated wavenumber is listed. In the 2–1 band some perturbations were observed in the  $F_1$  and  $F_2$  components of the  $v = 2$  level of the  $d^3\Pi_g$  state. The spectral lines in the vicinity of the perturbed region were deweighted in the fit.

The  $T_v$  and  $B_v$ -values of Tables 3 and 4 were fitted to the usual polynomial expressions (Herzberg 1950) in powers of  $(v + \frac{1}{2})$  to obtain sets of equilibrium parameters. From these fits the parameters  $\omega_e$ ,  $\omega_e x_e$ , and  $\omega_e y_e$ ,  $B_e$  and  $\alpha_e$  were obtained for

TABLE 3  
MOLECULAR CONSTANTS (IN  $\text{cm}^{-1}$ ) FOR THE  $a^3\Pi_u$  STATE OF THE  $\text{C}_2$  MOLECULE

Molecular Constant	$v = 0$	$v = 1$	$v = 2$	$v = 3$	$v = 4$
$T_v$ .....	0.0	1618.02017(52)	3212.7212(15)	4784.0929(35)	6332.1250(68)
$A_v$ .....	-15.26960(34)	-15.25173(49)	-15.2382 <sup>a</sup>	-15.2167 <sup>a</sup>	-15.1986 <sup>a</sup>
$A_{Dv} \times 10^4$ .....	2.503(57)	2.005(59)	2.0 <sup>b</sup>	2.0 <sup>b</sup>	2.0 <sup>b</sup>
$B_v$ .....	1.6240529(39)	1.6074280(37)	1.590799(60)	1.57432(15)	1.55677(42)
$D_v \times 10^6$ .....	6.4567(21)	6.4447(19)	6.4607 <sup>a</sup>	6.4772 <sup>a</sup>	6.5001 <sup>a</sup>
$H_v \times 10^{12}$ .....	7.85(24)	...	...	...	...
$q_v \times 10^4$ .....	-5.245(37)	-5.816(34)	-5.6 <sup>b</sup>	-5.6 <sup>b</sup>	-5.6 <sup>b</sup>
$q_{Dv} \times 10^8$ .....	-1.288(47)	...	...	...	...
$p_v \times 10^3$ .....	2.457(37)	2.720(37)	2.6 <sup>b</sup>	2.6 <sup>b</sup>	2.6 <sup>b</sup>
$p_{Dv} \times 10^7$ .....	1.20(20)	...	...	...	...
$o_v$ .....	0.67533(28)	0.66982(41)	0.6600(49)	0.6668(62)	0.66 <sup>b</sup>
$o_{Dv} \times 10^6$ .....	-8.23(83)	...	...	...	...
$\lambda_v$ .....	-0.15450(27)	-0.15327(39)	-0.15 <sup>b</sup>	-0.15 <sup>b</sup>	-0.15 <sup>b</sup>

<sup>a</sup> Held fixed to the value reported by Davis et al. 1988a.<sup>b</sup> Held fixed in the fit; see text for details.

TABLE 4  
MOLECULAR CONSTANTS (IN  $\text{cm}^{-1}$ ) FOR THE  $d^3\Pi_g$  STATE OF THE  $\text{C}_2$  MOLECULE

Molecular Constant	$v = 0$	$v = 1$	$v = 2$	$v = 3$
$T_v$ .....	19378.46141(50)	21132.13932(20)	22848.3908(14)	24524.2080(25)
$A_v$ .....	-14.00090(51)	-13.87387(38)	-13.8206(15)	-13.5233(23)
$A_{Dv} \times 10^4$ .....	4.774(68)	5.519(66)	5.2 <sup>a</sup>	5.2 <sup>a</sup>
$B_v$ .....	1.7455665(37)	1.7254184(45)	1.704340(20)	1.681445(67)
$D_v \times 10^6$ .....	6.8204(16)	7.0277(55)	7.106(26)	7.374(33)
$q_v \times 10^4$ .....	-7.804(35)	-8.139(36)	-6.510(97)	-7.51(10)
$p_v \times 10^3$ .....	3.976(37)	4.078(36)	4.0 <sup>a</sup>	4.0 <sup>a</sup>
$o_v$ .....	0.61072(42)	0.61705(28)	0.6228(23)	0.5746(57)
$\lambda_v$ .....	0.03331(38)	0.02976(28)	0.03 <sup>a</sup>	0.03 <sup>a</sup>

<sup>a</sup> Held fixed in the fit; see text for details.

the  $a^3\Pi_u$  and  $d^3\Pi_g$  states. The parameter  $\gamma_e$  was also estimated for the  $d^3\Pi_g$  state. All these parameters are listed in Table 5 along with one standard deviation error. The equilibrium vibrational constants  $\omega_e$ ,  $\omega_e x_e$ , and  $\omega_e y_e$  for the  $d^3\Pi_g$  state were obtained from an exact fit of the  $T_v$  ( $v = 0$  to 3) values. Hence no standard deviations are reported for these parameters. When only the  $\omega_e$  and  $\omega_e x_e$  were estimated from these term values, the fit was not very good and it was essential to estimate  $\omega_e y_e$ , even though the data were limited. The  $B_e$ -values were used to estimate the equilibrium internuclear distance,  $r_e$ , for the  $a$  and  $d$  states. These values are also listed in the same table. Note that the presence of extensive local and global perturbations in the  $d^3\Pi_g$  state make the determination of equilibrium constants difficult without a complete deperturbation.

## 5. SUMMARY

The jet expansion source is very useful for recording spectra of free radicals of astronomical interest. The low rotational temperatures simulate the conditions found in interstellar space. The usefulness of the jet source is demonstrated by comparing the spectrum recorded using this source with that obtained with a more conventional hollow cathode source. The wavenumber data obtained in the present work were combined with the most recently available data in the literature and an improved set of molecular constants was obtained for the first few vibrational levels of the  $d^3\Pi_g$  and  $a^3\Pi_u$  states involved in the Swan system of the  $\text{C}_2$  molecule. The molecular constants and line positions reported in this paper may prove useful to astronomers and other scientists observing  $\text{C}_2$  in energetic environments.

TABLE 5  
EQUILIBRIUM MOLECULAR CONSTANTS FOR THE  $a^3\Pi_u$  AND  $d^3\Pi_g$  STATES OF  $\text{C}_2$

Molecular Constant <sup>a</sup>	$a^3\Pi_u$	$d^3\Pi_g$
$\omega_e$ .....	1641.32959(3)	1788.22201 <sup>b</sup>
$\omega_e x_e$ .....	11.651954(18)	16.457464 <sup>b</sup>
$\omega_e y_e$ .....	-0.0016947(30)	-0.5012829 <sup>b</sup>
$B_e$ .....	1.6323654(73)	1.755234(97)
$\alpha_e$ .....	0.0166250(64)	0.01907(19)
$\gamma_e \times 10^3$ .....	...	-0.535(81)
$r_e(\text{\AA})$ .....	1.3119399(30)	1.265188(35)

<sup>a</sup> Constants are in  $\text{cm}^{-1}$  units unless stated otherwise.<sup>b</sup> This is an exact fit; see text for details.

The National Solar Observatory is operated by the Association for Research in Astronomy, Inc., under contract with the National Science Foundation. We thank J. Wagner, C. Plymate and G. Ladd for assistance in recording the spectra. We also thank R. W. Nicholls for providing the reference Tyte et al. (1967). This work was supported by the NASA Origins of the Solar System Research Program and the Natural Sciences and Engineering Research Council of Canada (NSERC). Some support was provided by the Phillips Laboratory/Propulsion Directorate, Edwards Air Force Base, CA.

## REFERENCES

- Adams, W. S. 1941, *ApJ*, 93, 11  
 Arniot, C. 1983, *ApJS*, 52, 329  
 Black, J. H., & van Dishoeck, E. F. 1988, *ApJ*, 331, 986  
 Brault, J. W., Delbouille, L., Grevesse, N., Roland, G., Sauval, A. J., & Testerman, K. 1982, *A&A*, 108, 201  
 Brazier, C. R., Ram, R. S., & Bernath, P. F. 1986, *J. Molec. Spectrosc.*, 120, 381  
 Brown, J. M., & Merer, A. J. 1979, *J. Molec. Spectrosc.*, 74, 488  
 Budó, A. 1936, *Z. Phys.*, 98, 437  
 Burgrim, E. D., Lyutyi, A. I., Rossikhin, V. S., & Tiskora, I. L. 1965, *Opt. Spectrosc.*, 19, 292  
 Chaffee, F. H., Jr., & Lutz, B. L. 1978, *ApJ*, 221, L91  
 Chaffee, F. H., Jr., Lutz, B. L., Black, J. H., Vanden Bout, P. A., & Snell, R. L. 1980, *ApJ*, 236, 474  
 Ciccone, A. 1942, *Nuovo Cimento*, 19, 1  
 Crane, P., Hegyi, D. J., Mandolesi, N., & Danks, A. C. 1986, *ApJ*, 309, 822  
 Curtis, M. C., & Sarre, P. J. 1985, *J. Molec. Spectrosc.*, 114, 427  
 ———. 1988, *Molec. Phys.*, 65, 225  
 Danks, A. C., Lambert, D. L., & Arpigny, C. 1974, *ApJ*, 194, 745  
 Davis, S. P., Abrams, M. C., Phillips, J. G., & Rao, M. L. P. 1988b, *J. Opt. Soc. Am. B*, 5, 2280  
 Davis, S. P., Abrams, M. C., Sandalphon, Brault, J. W., & Rao, M. L. P. 1988a, *J. Opt. Soc. Am. B*, 5, 1838  
 Douay, M., Nietmann, R., & Bernath, P. F. 1988a, *J. Molec. Spectrosc.*, 131, 250  
 ———. 1988b, *J. Molec. Spectrosc.*, 131, 261  
 Engelking, P. C. 1986, *Rev. Sci. Instr.*, 57, 2274  
 Federman, S. R., Danks, A. C., & Lambert, D. L. 1984, *ApJ*, 287, 219  
 Federman, S. R., & Huntress, W. T. 1989, *ApJ*, 338, 140  
 Gerin, M., Combes, F., Encrenaz, P., Linke, R., Destombes, J. L., & Demuync, C. 1984, *A&A*, 136, L17  
 Goebel, J. H., Bregman, J. D., Cooper, D. M., Goorvitch, D., Langhoff, S. R., & Witteborn, F. C. 1983, *ApJ*, 270, 190  
 Gredel, R., van Dishoeck, E. F., & Black, J. H. 1989, *ApJ*, 338, 1047  
 Grevesse, N., & Sauval, A. J. 1973, *A&A*, 27, 29  
 Herzberg, G. 1946, *Phys. Rev.*, 70, 752  
 ———. 1950, *Spectra of Diatomic Molecules* (New York: Van Nostrand Reinhold)  
 Hobbs, L. M. 1979, *ApJ*, 232, L175  
 ———. 1981, *ApJ*, 243, 485  
 Hobbs, L. M., Black, J. H., & van Dishoeck, E. F. 1983, *ApJ*, 271, L95  
 Hobbs, L. M., & Campbell, B. 1982, *ApJ*, 254, 108  
 Huber, K. P., & Herzberg, G. 1979, *Constants of Diatomic Molecules* (New York: Van Nostrand Reinhold)  
 Johnson, J. R., Fink, U., & Larson, H. P. 1983, *ApJ*, 270, 769  
 Johnson, R. C. 1927, *Phil. Trans. R. Soc. Lond.*, A, 226, 157  
 Johnson, R. C., & Asundi, R. K. 1992, *Phil. Trans. R. Soc. Lond.*, A, 342, 668  
 Kakimoto, M., & Kasuya, Y. 1982, *J. Molec. Spectrosc.*, 94, 380  
 King, A. S., & Birge, R. T. 1930, *ApJ*, 72, 19  
 Lambert, D. L. 1968, *MNRAS*, 138, 143  
 ———. 1978, *MNRAS*, 182, 249  
 Lambert, D. L., Brown, J. A., Hinkle, K. H., & Johnson, H. R. 1984, *ApJ*, 284, 223  
 Lambert, D. L., & Danks, A. C. 1983, *ApJ*, 268, 248  
 Lambert, D. L., Sheffer, Y., & Crane, P. 1990, *ApJ*, 359, L19  
 Li, Z., & Francisco, J. S. 1992, *J. Chem. Phys.*, 96, 878  
 Mayer, P., & O'Dell, C. R. 1968, *ApJ*, 153, 951  
 McKellar, A. 1940, *PASP*, 52, 187  
 ———. 1941, *Publ. Dom. Astrophys. Obs Victoria*, 7, 251  
 Mecke, R. 1925, *Z. Phys.*, 26, 217  
 Meyer, D. M., & Jura, M. 1984, *ApJ*, 276, L1  
 ———. 1985, *ApJ*, 297, 119  
 Meyer, D. M., Roth, K. C., & Hawkins, I. 1989, *ApJ*, 343, L1  
 Morton, D. C. 1975, *ApJ*, 197, 85  
 Mulliken, R. S. 1927, *Phys. Rev.*, 29, 637  
 ———. 1929, *Phys. Rev.*, 33, 507  
 Norlen, G. 1973, *Phys. Scripta*, 8, 249  
 Oliphant, N., Lee, A., Bernath, P. F., & Brazier, C. R. 1990, *J. Chem. Phys.*, 92, 2244  
 Penzias, A. A., Jefferts, K. B., & Wilson, R. W. 1972, *Phys. Rev. Lett.*, 28, 772  
 Phillips, J. G. 1948, *ApJ*, 108, 434  
 ———. 1968, *J. Molec. Spectrosc.*, 28, 233  
 Phillips, J. G., & Davis, S. P. 1968, *The Berkeley Analysis of Molecular Spectra*, Vol. 2, *The Swan System of the C<sub>2</sub> Molecule and the Spectrum of the HgH Molecule* (Berkeley: Univ. California)  
 Prasad, C. V. V., & Bernath, P. F. 1992, *J. Molec. Spectrosc.*, 156, 327  
 Prasad, C. V. V., Bernath, P. F., Frum, C., & Engleman, R., Jr. 1992, *J. Molec. Spectrosc.*, 151, 459  
 Querci, F., Querci, M., & Kunde, V. G. 1971, *A&A*, 15, 256  
 Rehfuss, B. D., Suh, M. H., Miller, T. A., & Bondybey, V. E. 1992, *J. Molec. Spectrosc.*, 151, 437  
 Richard, E. C., Donaldson, D. J., & Vaida, V. 1989, *Chem. Phys. Lett.*, 157, 295  
 Shea, J. D. 1927, *Phys. Rev.*, 30, 825  
 Sneden, C., & Lambert, D. L. 1982, *ApJ*, 259, 381  
 Souza, S. P., & Lutz, B. L. 1977, *ApJ*, 216, L49  
 Stawikowski, A., & Greenstein, J. L. 1964, *ApJ*, 140, 1280  
 Suzuki, T., Saito, S., & Hirota, E. 1985, *J. Molec. Spectrosc.*, 113, 399  
 Swan, W. 1857, *Trans. R. Soc. Edinburgh*, 21, 411  
 Thaddeus, P. 1972, *ARA&A*, 10, 305  
 Turner, B. E., & Gammon, R. H. 1975, *ApJ*, 198, 71  
 Tyte, D. C., Innanen, S. H., & Nicholls, R. W. 1967, *Identification Atlas of Molecular Spectra*, Vol. 5, *The C<sub>2</sub> d<sup>3</sup>Π<sub>g</sub>-a<sup>3</sup>Π<sub>u</sub> Swan System* (Toronto: Centre for Research in Experimental Space Science)  
 van Dishoeck, E. F., & de Zeeuw, T. 1984, *MNRAS*, 206, 383  
 Wollaston, W. H. 1802, *Phil. Trans. R. Soc. Lond.*, 11, 365  
 Wooten, A., Lichten, S. M., Sahai, R., & Wannier, P. G. 1982, *ApJ*, 257, 151